

# Magnetic ‘Molecular Oligomers’ Based on Decametalllic Supertetrahedra: A Giant Mn<sub>49</sub> Cuboctahedron and its Mn<sub>25</sub>Na<sub>4</sub> Fragment

Maria Manoli,<sup>a</sup> Sofia Alexandrou,<sup>a</sup> Linh Pham,<sup>b,‡</sup> Giulia Lorusso,<sup>c</sup> Wolfgang Wernsdorfer,<sup>d</sup> Marco Evangelisti,<sup>c</sup> George Christou,<sup>b</sup> and Anastasios J. Tasiopoulos<sup>a\*</sup>

**Abstract:** Two nanosized Mn clusters, [Mn<sub>49</sub>(O)<sub>32</sub>(OCH<sub>3</sub>)<sub>8</sub>(hp)<sub>24</sub>(O<sub>2</sub>CH)<sub>6</sub>(DMF)<sub>12</sub>(OH)<sub>8</sub> (**1**) and [Mn<sub>25</sub>Na<sub>4</sub>(O)<sub>16</sub>(OCH<sub>3</sub>)<sub>4</sub>(hp)<sub>16</sub>(O<sub>2</sub>CCH<sub>3</sub>)<sub>4</sub>(O<sub>2</sub>CH)(DMF)<sub>8</sub>(O<sub>2</sub>CH) (**2**) (H<sub>2</sub>hp = 2-(Hydroxymethyl)phenol) based on analogues of the high spin (*S* = 22) [Mn<sup>III</sup><sub>6</sub>Mn<sup>II</sup><sub>4</sub>(μ<sub>4</sub>-O)<sub>4</sub>]<sup>18+</sup> supertetrahedral core are reported. Complexes **1** and **2** consist of eight and four decametalllic supertetrahedral subunits, respectively, display high (O<sub>h</sub>) virtual symmetry and represent unique examples of clusters based on a large number of tightly linked high nuclearity magnetic units. They also possess dominant ferromagnetic exchange interactions and large spin ground state values *S* = 6<sup>1</sup>/<sub>2</sub> (**1**) and 5<sup>1</sup>/<sub>2</sub> (**2**) with the Mn<sub>49</sub> cluster displaying single molecule magnetism (SMM) behavior and being the second largest homometallic SMM.

The construction of giant metal clusters based on tightly connected, magnetically interesting, polynuclear complexes is one of the most important challenges for coordination chemists. Interest in such compounds stems not only from their impressive structural features such as large size, high symmetry, beautiful shapes and architectures, but also from the possibility that the magnetic properties of their structural subunits to be retained or even enhanced in the large polynuclear assembly. Although several giant metal organic compounds have been reported, the structures of both the homometallic (e.g. Mn<sub>84</sub>,<sup>[1]</sup> Mn<sub>44</sub>,<sup>[2]</sup> Mn<sub>32</sub>,<sup>[3-5]</sup> Fe<sub>64</sub>,<sup>[6]</sup> Fe<sub>42</sub>,<sup>[7]</sup> Co<sub>36</sub>,<sup>[8]</sup> Cu<sub>44</sub>,<sup>[9]</sup> Pd<sub>84</sub>,<sup>[10]</sup> and Ln<sub>104</sub> (Ln = Nd, Gd)<sup>[11]</sup>) and heterometallic (e.g. Mn<sub>36</sub>Ni<sub>4</sub>,<sup>[12]</sup> Cu<sub>17</sub>Mn<sub>28</sub>,<sup>[13]</sup> [Ni<sub>12</sub>(Cr<sub>7</sub>Ni)<sub>6</sub>],<sup>[14]</sup> Ni<sub>60</sub>La<sub>76</sub>,<sup>[15]</sup> Ni<sub>54</sub>Gd<sub>54</sub>,<sup>[16]</sup> Cu<sub>36</sub>Ln<sub>24</sub> (Ln = Gd, Dy),<sup>[17]</sup>) ones contain mainly oligonuclear, usually trinuclear (e.g. oxo or hydroxy-shaped triangles) and tetranuclear (e.g. cubanes) subunits. There are also a few examples of nanosized clusters based on subunits that have not been isolated in discrete form and only a couple of complexes displaying building units or fragments that have been reported in the literature. Such examples are the Fe<sub>64</sub> cluster based on an Fe<sub>8</sub> subunit<sup>[6]</sup> and the Mn<sub>84</sub> wheel which

contain a Mn<sub>11</sub> fragment reported in the past, although its true repeating unit is a Mn<sub>14</sub> cluster never seen in discrete form.<sup>[1]</sup> Despite the fact that the synthesis of most of the giant metal-organic clusters is a very complicated process based to some extent on serendipity, a discussion has been initiated in the scientific community concerning the possibility to predict the structure and nuclearity of metal-organic clusters that could be targeted and prepared by future generations of chemists.<sup>[10,18]</sup> It would be tempting to assume for example that stable structural units easily assembled in the reaction solution under various conditions could be linked in the presence of the proper bridging ligands giving rise to a library of theoretically predicted high nuclearity clusters. However, so far there is no experimental proof to support this expectation.

One ideal structural type to act as a building – block in high nuclearity clusters is the [Mn<sup>III</sup><sub>6</sub>Mn<sup>II</sup><sub>4</sub>(μ<sub>4</sub>-O)<sub>4</sub>]<sup>18+</sup> supertetrahedral core which combines a beautiful, high symmetry (T<sub>d</sub>) metal topology and interesting magnetic properties.<sup>[19]</sup> In addition, it has been stabilized in discrete form with several ligands<sup>[19-21]</sup> and under various reaction conditions, and has appeared as the repeating unit in 0-D Mn<sub>17</sub>,<sup>[22,23]</sup> and Mn<sub>19</sub>,<sup>[24]</sup> clusters and in the giant Mn<sub>36</sub>Ni<sub>4</sub> “loop – of – loops and supertetrahedra” aggregate,<sup>[12]</sup> all containing two Mn<sup>III</sup><sub>6</sub>Mn<sup>II</sup><sub>4</sub> supertetrahedral units. Most of the compounds possessing this core display ferromagnetic exchange interactions and large or even giant ground state spin values which for the Mn<sub>10</sub>, Mn<sub>17</sub>, Mn<sub>19</sub> and Mn<sub>36</sub>Ni<sub>4</sub> clusters mentioned above are *S* = 22, 37, 83<sup>1</sup>/<sub>2</sub> and 26, respectively. However, there is no cluster containing more than two Mn<sup>III</sup><sub>6</sub>Mn<sup>II</sup><sub>4</sub> supertetrahedral subunits.

Herein we report compounds [Mn<sup>III</sup><sub>36</sub>Mn<sup>II</sup><sub>13</sub>(μ<sub>4</sub>-O)<sub>32</sub>(μ<sub>3</sub>-OCH<sub>3</sub>)<sub>8</sub>(μ<sub>3</sub>-hp)<sub>24</sub>(O<sub>2</sub>CH)<sub>6</sub>(DMF)<sub>12</sub>(OH)<sub>8</sub> (**1**) and [Mn<sup>III</sup><sub>20</sub>Mn<sup>II</sup><sub>5</sub>Na<sub>4</sub>(μ<sub>4</sub>-O)<sub>16</sub>(μ<sub>3</sub>-OCH<sub>3</sub>)<sub>4</sub>(μ<sub>3</sub>-hp)<sub>16</sub>(O<sub>2</sub>CCH<sub>3</sub>)<sub>4</sub>(O<sub>2</sub>CH)(DMF)<sub>8</sub>(O<sub>2</sub>CH) (**2**) (H<sub>2</sub>hp = 2-(Hydroxymethyl)phenol) consisting of eight and four fused M<sub>10</sub> supertetrahedral units respectively. Both compounds display highly symmetric, nanosized structural cores (O<sub>h</sub> virtual symmetry) with that of **1** describing an “Archimedean solid” called a cuboctahedron. In addition, they are structurally related, with the core of **2** being almost identical to a fragment of that of **1**. Magnetism studies revealed the existence of dominant ferromagnetic exchange interactions in both **1** and **2** leading to ground state spin values of 6<sup>1</sup>/<sub>2</sub> and 5<sup>1</sup>/<sub>2</sub> respectively. In addition, the magnetocaloric effect for both complexes is seen to develop over a significantly wide temperature range. Finally, compound **1** displays SMM behavior being the second largest homometallic 3d SMM reported in the literature.

Both compounds discussed herein were prepared from the investigation of reactions of Mn salts with 2-(hydroxymethyl)phenol (H<sub>2</sub>hp) under various conditions. Thus, the reaction of [Mn(ClO<sub>4</sub>)<sub>2</sub>]·xH<sub>2</sub>O, H<sub>2</sub>hp, NaOCN and Bu<sub>4</sub>N(ClO<sub>4</sub>) in a 1:1:1:1 molar ratio in DMF/MeOH solvent mixture led to the isolation of 1·10DMF in 20 % yield after ~ 2 months. Compound 2·DMF was isolated in ~25% yield from the reaction of

[a,\*] Dr. M. Manoli, Mrs S. Alexandrou, Dr. A. J. Tasiopoulos  
Department of Chemistry, University of Cyprus, 1678 Nicosia, Cyprus  
E-mail: atasio@ucy.ac.cy

[b] Dr. L. Pham, ‡ Prof. G. Christou  
Department of Chemistry, University of Florida, Gainesville, Florida 32611-7200  
‡Current address: Texas A&M University-Central Texas, Department of Science and Mathematics, Killeen, TX 76549

[c] Dr. G. Lorusso, Dr. M. Evangelisti  
Instituto de Ciencia de Materiales de Aragón and Departamento de Física de la Materia Condensada, CSIC-Universidad de Zaragoza, 50009 Zaragoza, Spain

[d] Dr. W. Wernsdorfer  
Institut Neel, CNRS, BP 166, 25 Avenue des Martyrs, 38042 Grenoble Cedex 9, France.

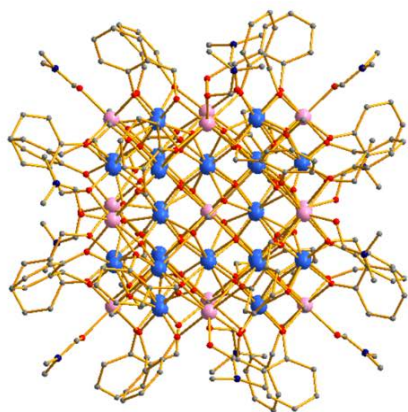
Mn(acac)<sub>2</sub> with H<sub>2</sub>hp in the presence of NaOMe in a 1:1:2 molar ratio in a DMF/MeOH solvent mixture. Some of the chemicals used in the reaction mixture resulting in **1** do not appear in the final product, however their presence in the reaction mixture is essential for the isolation of the compound since the latter is not formed when the reaction is repeated without their use. It should also be pointed out that although both compounds are prepared in moderate yields after several weeks, their synthesis is reproducible.

The asymmetric unit of **1**<sup>[25]</sup> consists of two independent quarters of the Mn<sub>49</sub> cation (Figure 1a) and also OH<sup>-</sup> counter-ions and solvents of crystallization. The two Mn<sub>49</sub> units are nearly identical including a centrosymmetric, mixed-valent [(Mn<sup>III</sup><sub>36</sub>Mn<sup>II</sup><sub>13</sub>(μ<sub>4</sub>-O)<sub>32</sub>]<sup>70+</sup> structural core (Figure 1b). The latter consists of eight [Mn<sup>III</sup><sub>6</sub>Mn<sup>II</sup><sub>4</sub>(μ<sub>4</sub>-O)<sub>4</sub>]<sup>18+</sup> supertetrahedral subunits (Figure 1b, right) all having a common apex Mn<sup>II</sup> ion and each of them sharing three edges with three other neighbouring supertetrahedra. The assembly of the eight Mn<sub>10</sub> supertetrahedra results in a geometrical 3-D shape consisting of 6 square pyramids sharing their triangular faces with eight tetrahedra. The Mn<sub>49</sub> polyhedron thus has 8 triangular and 6 square faces and describes an "Archimedean solid" called a cuboctahedron (Figure 1c). The 12 Mn<sup>2+</sup> ions define the vertices of the cuboctahedron and 24 Mn<sup>3+</sup> ions are located on its edges. The rest of the Mn<sup>3+</sup> (twelve) and Mn<sup>2+</sup> (one) ions of **1** are found on the inner edges of the supertetrahedra and at the centre of the cuboctahedron, respectively. The μ<sub>4</sub>-O<sup>2-</sup> ions of the Mn<sub>49</sub> cluster bridge 3Mn<sup>3+</sup> and one Mn<sup>2+</sup> ions, as has been seen in other structures containing the [Mn<sup>III</sup><sub>6</sub>Mn<sup>II</sup><sub>4</sub>(μ<sub>4</sub>-O)<sub>4</sub>]<sup>18+</sup>

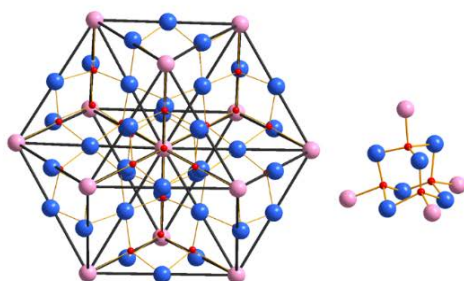
supertetrahedral core whereas the μ<sub>3</sub>-MeO<sup>-</sup> ligands bridge three Mn<sup>3+</sup> ions. The peripheral ligation is completed by 24 fully deprotonated hp<sup>2-</sup> ligands connecting two Mn<sup>2+</sup> and one Mn<sup>3+</sup> ions in a η<sup>2</sup>:η<sup>2</sup>-μ<sub>3</sub> mode, six severely disordered HCO<sub>2</sub><sup>-</sup> ligands bridging exclusively Mn<sup>3+</sup> ions, and 12 terminal DMF molecules bound to the 12 outer Mn<sup>2+</sup> ions.

The asymmetric unit of **2**·DMF<sup>[25]</sup> consists of one quarter of the cation of **2** (Figure 2a) and lattice counter-ions and solvent molecules. Its [Mn<sup>III</sup><sub>20</sub>Mn<sup>II</sup><sub>5</sub>Na<sub>4</sub>(μ<sub>4</sub>-O)<sub>16</sub>]<sup>42+</sup> core (Figure 2b) consists of four [Mn<sup>III</sup><sub>6</sub>Mn<sup>II</sup><sub>3</sub>Na(μ<sub>4</sub>-O)<sub>4</sub>]<sup>17+</sup> supertetrahedral units having a common Mn<sup>II</sup> ion occupying their apex position and each of them sharing two edges with two other neighbouring supertetrahedra. The overall shape of the core can be described as a square pyramid sharing each of its triangular faces with a supertetrahedron. The Mn<sup>II</sup> ions occupy the common vertices of the square pyramid and the supertetrahedra and the Na<sup>+</sup> ions the remaining vertices of the four supertetrahedra. Sixteen Mn<sup>3+</sup> ions are located on the outer edges of the four supertetrahedra and four on their inner edges (in the common faces of the square pyramid and the four supertetrahedra). The described core of **2** is related to that of **1** in being almost equal to a fragment of the latter. In fact, the core of **1** can be described as consisting of two M<sub>29</sub> units of **2** sharing a central M<sub>9</sub> plane (Figure 3). As a result, structural features such as the bridging modes of the ligands, the coordination environment and number of metal ions, etc in **2** are similar to those described for **1**. Thus, each of the sixteen O<sup>2-</sup> ions of the core is linked to three Mn<sup>3+</sup> and one Mn<sup>2+</sup> or Na<sup>+</sup> ions, the four MeO<sup>-</sup> groups to three Mn<sup>3+</sup> ions, and

a)



b)



c)

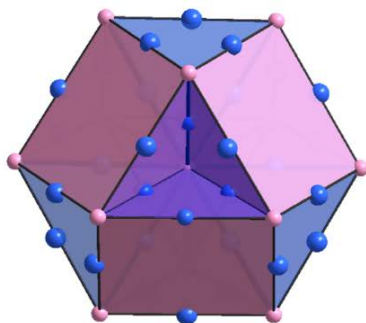


**Figure 1.** Representations of the a) molecular structure of the cation of **1**, b)  $[\text{Mn}^{\text{II}}_{36}\text{Mn}^{\text{III}}_{13}(\mu_4\text{-O})_{32}]^{70+}$  structural core (left), and  $[\text{Mn}^{\text{III}}_6\text{Mn}^{\text{II}}_4(\mu_4\text{-O})_4]^{18+}$  supertetrahedral subunit (right) and c)  $\text{Mn}_{49}$  metallic skeleton; the solid lines connecting the Mn ions in Figs. b (left) and c and the coloured planes in Fig. c are used to emphasize the existence of eight  $\text{Mn}^{\text{III}}_6\text{Mn}^{\text{II}}_4$  supertetrahedral subunits, and the cuboctahedral shape of the structural core and the metallic skeleton. Colour code:  $\text{Mn}^{\text{III}}$  blue;  $\text{Mn}^{\text{II}}$  pink; O red; N dark blue; C grey.

the sixteen  $\text{hp}^2$  ligands bridge in a  $\eta^2:\eta^2-\mu_3$  mode either  $\text{Mn}^{2+}/\text{Na}^+/\text{Mn}^{3+}$  or  $2\text{Mn}^{2+}/\text{Mn}^{3+}$  ions. The peripheral ligation is completed by four acetate ligands bridging in a  $\eta^1:\eta^3-\mu_4$  mode, a severely disordered formate ion, and eight terminal DMF molecules connected to the  $\text{Mn}^{2+}$  and  $\text{Na}^+$  ions.

The oxidation states of the Mn ions and the protonation level of  $\text{O}^{2-}/\text{RO}^-$  ligands in **1** and **2** were determined by BVS calculations, charge considerations and inspection of metric parameters.<sup>[26,27]</sup> All octahedral  $\text{Mn}^{3+}$  ions display a JT elongation with the carboxylate O and  $\mu_3\text{-MeO}^-$  being located on the JT axes, which however are not co-parallel.

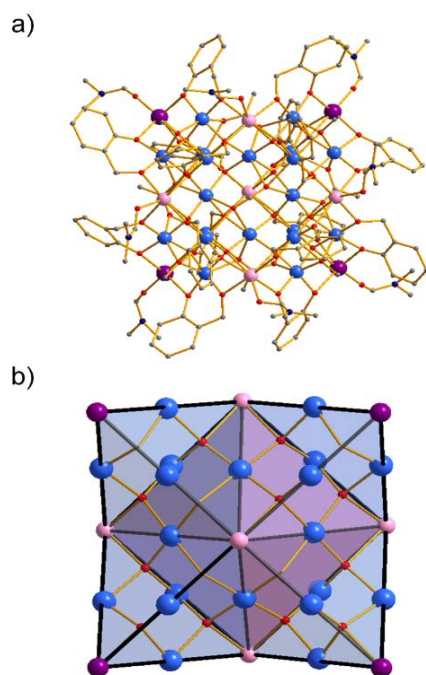


**Figure 2.** Representations of the a) molecular structure of the cation of **2** and b)  $[\text{Mn}^{\text{III}}_{20}\text{Mn}^{\text{II}}_5\text{Na}_4(\mu_4\text{-O})_{16}]^{42+}$  structural core; the coloured planes in Fig 2b and the solid black lines connecting the Mn ions are used to emphasize the description of the core of **1** as a square pyramid sharing its triangular faces with four tetrahedra, and also the presence of the four  $[\text{Mn}^{\text{III}}_6\text{Mn}^{\text{II}}_3\text{Na}(\mu_4\text{-O})_4]^{17+}$  supertetrahedral subunits. Colour code:  $\text{Mn}^{\text{III}}$  blue;  $\text{Mn}^{\text{II}}$  pink;  $\text{Na}^+$  purple; O red; N dark blue; C grey.

Interestingly, the cores of **1** and **2** are also related to the  $[\text{Mn}^{\text{III}}_{11}\text{Mn}^{\text{II}}_6(\mu_4\text{-O})_8]^{29+}$  core of a family of  $\text{Mn}_{17}$  clusters reported

recently, (see Figure 3 and Figure S4 in the supporting information).<sup>[22,23]</sup> The latter consists of two edge-sharing  $[\text{Mn}^{\text{III}}_6\text{Mn}^{\text{II}}_4(\mu_4\text{-O})_4]^{18+}$  supertetrahedral units, displays ferromagnetic exchange interactions with one of the  $\text{Mn}_{17}$  analogues combining an  $S = 37$  spin ground state and SMM behaviour being the highest spin SMM.<sup>[22]</sup> Complex **2** contains two  $[\text{Mn}^{\text{III}}_{11}\text{Mn}^{\text{II}}_6(\mu_4\text{-O})_8]^{29+}$  fragments, nearly identical to the core of the above discussed  $\text{Mn}_{17}$  cluster, sharing a  $M_5$  plane, whereas complex **1** consists of four such units sharing two  $M_5$  planes with the neighbouring ones. Both **1** and **2** are nanosized clusters and among the largest discrete (0-D) 3d metal clusters with maximum dimensions of  $\sim 2.5$  and  $2.2$  nm and molecular weights of  $\sim 8400$  and  $\sim 4800$  g/mol, respectively, with the former one being smaller only from  $\text{Mn}_{84}$  and  $\text{Fe}_{64}$  clusters.<sup>[1,6]</sup>

Direct current magnetic susceptibility ( $\chi_M$ ) measurements were performed on powdered crystalline samples of **1**:DMF and **2**:DMF in the 5 - 300 K temperature range in a 0.1 T magnetic field. The data are plotted as  $\chi_M T$  vs.  $T$  in Figure 4a.  $\chi_M T$  for **1**:DMF and **2**:DMF increases steadily from 189.6 and 101.4  $\text{cm}^3 \text{mol}^{-1} \text{K}$ , respectively, at 300 K to maxima of 536.8 (at 20 K) and 367.2  $\text{cm}^3 \text{mol}^{-1} \text{K}$  (at 10 K) before decreasing to 431.5 and 337.9  $\text{cm}^3 \text{mol}^{-1} \text{K}$  at 5.0 K. The 300 K values of both compounds are higher than the spin-only ( $g = 2$ ) values of 164.875  $\text{cm}^3 \text{mol}^{-1} \text{K}$  for 13  $\text{Mn}^{\text{II}}$  and 36  $\text{Mn}^{\text{III}}$  and 81.875  $\text{cm}^3 \text{mol}^{-1} \text{K}$  for 5  $\text{Mn}^{\text{II}}$  and 20  $\text{Mn}^{\text{III}}$  non-interacting ions, indicating the

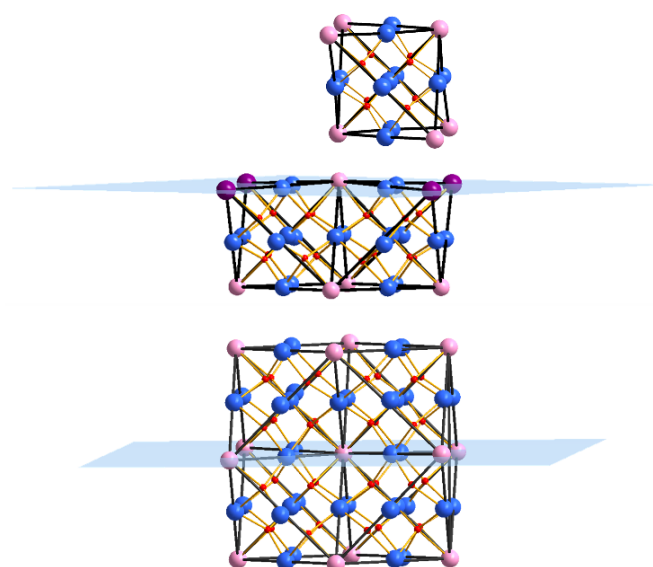


**Figure 3.** Representations of the structural cores of **1** (bottom), **2** (middle) and a  $\text{Mn}_{17}$  cluster known from the literature<sup>[22,23]</sup> (top, see text for details), respectively, highlighting their structural relationship; the light blue planes in the cores of **1** and **2** are used to emphasize the common  $M_5$  plane of the two  $\text{M}_{29}$  subunits, related to the structure of **2**, within the  $\text{M}_{49}$  cuboctahedral core of **1** (see the text for details). Colour code:  $\text{Mn}^{\text{III}}$  blue;  $\text{Mn}^{\text{II}}$  pink;  $\text{Na}^+$  purple; O red.

presence of dominant ferromagnetic exchange interactions within both molecules. The maximum  $\chi_M T$  values suggest ground-state spin ( $S$ ) values of approximately  $S = {}^{63}/_2 \pm 1$  (spin-only values 480.375, 511.875 and 544.375  $\text{cm}^3 \text{mol}^{-1} \text{K}$  for  $S = {}^{61}/_2, {}^{63}/_2$  and  ${}^{65}/_2$ , respectively) for **1**:DMF and  ${}^{53}/_2 \pm 1$  (spin-only values 337.875, 364.375 and 391.875  $\text{cm}^3 \text{mol}^{-1} \text{K}$  for  $S = {}^{51}/_2,$

$53/2$  and  $55/2$ , respectively) for **2-DMF**. The abrupt decrease of  $\chi_{\text{M}}T$  at very low  $T$  for both complexes is assigned to zero-field splitting (ZFS), Zeeman effects from the applied field, and/or weak inter-molecular interactions.

To further probe the ground-state spin, of the two complexes, magnetization ( $M$ ) vs dc field measurements at applied magnetic fields ( $H$ ) and temperatures in the 1-10 kG and 1.8-10.0 K ranges, respectively, were performed. The data are shown in Figures S9 and S10 for **1-10DMF** and **2-DMF**, respectively, as reduced magnetization ( $M/N\mu_{\text{B}}$ ) vs  $H/T$  plots, where  $N$  is Avogadro's number and  $\mu_{\text{B}}$  is the Bohr magneton. The data were fit by assuming that only the ground state is populated at these temperatures and magnetic fields, and by including isotropic Zeeman interactions and axial zero-field splitting ( $D\hat{S}_z^2$ ). Using only data collected at low fields to minimize problems from low-lying excited states, satisfactory fits were obtained (solid lines in Figures S9 and S10) with  $S = 61/2$ ,  $g = 1.99$  (1), and  $D = -0.01 \text{ cm}^{-1}$  for **1-10DMF**, and  $S = 51/2$ ,  $g = 1.99$  (1) and  $D = -0.01 \text{ cm}^{-1}$  for **2-DMF**. Alternative fits with slightly higher or lower  $S$  values gave for both compounds unreasonable values of  $g$  and  $D$ .

Prompted by the large magnetization values observed in both complexes, we performed magnetocaloric studies to investigate their cooling capability. A complete discussion about

$= 7 \text{ T}$  for **2-DMF** (Figure S8). Interestingly, the entropy changes remain almost constant from 30 K to 5 K ( $\mu_0\Delta H = 7 \text{ T}$ ), indicating that both compounds display cooling capability for a significantly wide range of temperatures. It is also notable that the zero-field entropies for both complexes (Figure S6) are consistent with the afore-discussed ground-state spin values. On basis of the magnetization data, assuming that only  $S = 61/2$  ( $S = 51/2$ ) is populated below 2 K for **1-10DMF** (**2-DMF**) would imply a value for the zero-field magnetic entropy at 2 K close to  $R\ln(2S+1) = 4.1R$  (4.0R), where  $R$  is the gas constant, as indeed observed (Figure S6).

Alternating current (ac) magnetic susceptibility measurements were performed in the 1.8 – 10 K temperature range in zero applied dc field and a 3.5 G ac field oscillating at 50 – 1000 Hz. The plots of the in-phase component of the ac susceptibility  $\chi'_{\text{M}}T$  versus  $T$  and the out-of-phase susceptibility  $\chi''_{\text{M}}$  versus  $T$  for **1-10DMF** and **2-DMF** are shown in Figures S11 and S12. Extrapolation of the  $\chi'_{\text{M}}T$  data from above  $\sim 6.0 \text{ K}$  to 0 K, at which point only the ground state will be populated, (avoiding the lower  $T$  data that will be affected by intermolecular dipolar interactions, etc) gives values of  $\sim 460$  and  $\sim 360 \text{ cm}^3 \text{ mol}^{-1} \text{ K}$ , which are consistent with  $S = 61/2 \pm 1$  and  $51/2 \pm 1$  ground states for **1-10DMF** and **2-DMF**, respectively, with  $g \approx 2.00$ , confirming the conclusions from the dc studies. The out-of-phase plot of **1-10DMF** displays weak  $\chi''_{\text{M}}$  signals below 2.6 K, suggestive of the presence of slow relaxation of the magnetization. No out-of-phase signals were observed for **2-DMF**.

Encouraged by the giant spin ground state value and the observation of out-of-phase signals in **1-10DMF** we carried out, using a micro-SQUID apparatus, single-crystal hysteresis studies to confirm that it indeed displays SMM behavior. The obtained magnetization versus dc field data at different temperatures and a fixed field sweep rate of 0.002 T/s are shown in Figure 4b, and at different scan rates and a constant  $T = 0.5 \text{ K}$  in Figure S13. Hysteresis loops appeared below 1 K whose coercivities increase with decreasing temperature and increasing field scan rates, as expected for SMMs. Thus, **1-10DMF** is a new SMM, with a blocking temperature of 1 K, above which no hysteresis is observed. The hysteresis loops do not contain any steps characteristic of quantum tunneling of the magnetization (QTM); however this is typical for higher nuclearity SMMs where the steps are smeared out due to various effects such as existence of low-lying excited states, intermolecular interactions, etc.<sup>[1,2]</sup> Magnetization vs time decay data were collected on a single crystal of **1-10DMF** to assess the magnetization relaxation dynamics, and the results are shown in Figure S14. These data were used to calculate the relaxation rates ( $1/\tau$ ;  $\tau$  is the lifetime) at the different temperatures and construct the Arrhenius plot shown as  $\tau$  vs  $1/T$  in Figure S15 based on the Arrhenius equation:

$$\tau = \tau_0 \exp(U_{\text{eff}}/kT) \quad (1)$$

where  $\tau_0$  is the pre-exponential factor,  $U_{\text{eff}}$  is the effective relaxation barrier and  $k$  is the Boltzmann constant. The Arrhenius equation is appropriate for a thermally activated Orbach process, the characteristic behaviour of a Mn-based SMM. The fit to the thermally activated region above  $\sim 0.1 \text{ K}$  gave  $\tau_0 = 7 \cdot 10^{-14} \text{ s}$  and  $U_{\text{eff}} = 19 \text{ K}$ . The small value of  $\tau_0$ , smaller than is typical for purely SMM behaviour, is assigned to the low-

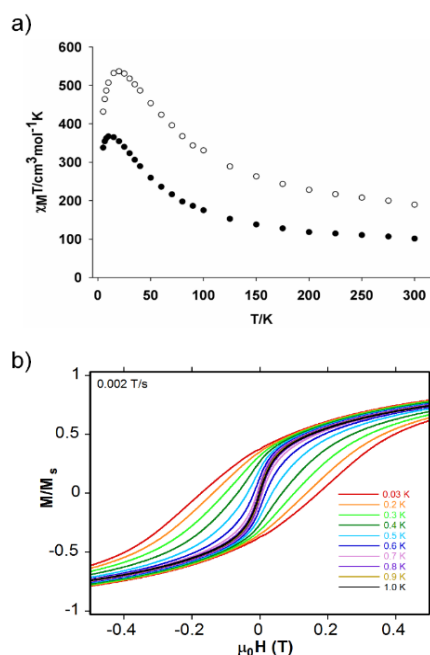


**Figure 4.** a)  $\chi_{\text{M}}T$  vs  $T$  plot for complex **1-10DMF** (open circles) and **2-DMF** (solid circles) at 0.1 T and b) magnetization ( $M$ ) vs applied magnetic field  $\mu_0 H$  hysteresis loops for a single crystal of **1-10DMF** at the indicated temperatures and a fixed field sweep rate of 0.002T/s. The magnetization is normalized to its saturation value ( $M_s$ ).

these investigations is provided in the supporting information. In comparison to the MCE reported for other molecular compounds,<sup>[28]</sup> the data revealed moderate entropy changes for both complexes, i.e.,  $-\Delta S_{\text{m}} = 6.4 \text{ J kg}^{-1} \text{ K}^{-1}$  at  $T = 10 \text{ K}$  and  $\mu_0\Delta H = 7 \text{ T}$  for **1-10DMF** and  $-\Delta S_{\text{m}} = 7.7 \text{ J kg}^{-1} \text{ K}^{-1}$  at  $T = 8 \text{ K}$  and  $\mu_0\Delta H$

lying excited states and the weak intermolecular interactions and is a common situation for large clusters.<sup>[2,22,23,29]</sup> At ~ 0.1 K and below the relaxation becomes temperature-independent as expected for relaxation by ground-state QTM, i.e. via the  $M_S = \pm 6^{1/2}$  levels of the  $S = 6^{1/2}$  spin manifold.

Summarizing, two nanosized  $Mn_{25}Na_4$  and  $Mn_{49}$  molecular aggregates based on four and eight  $[Mn^{II}_6Mn^{III}_3M(\mu_4-O)_4]^{n+}$  ( $M = Mn^{II}$ ,  $n = 18$ , **1**·10DMF;  $M = Na^+$ ,  $n = 17$ , **2**·DMF) supertetrahedral repeating units are reported. This extended conjunction of decametallc supertetrahedra afforded structural cores displaying high symmetry ( $O_h$ ) and aesthetically pleasing 3-D solid shapes including an Archimedean one, called a cuboctahedron. Compounds **1** and **2** also display dominant ferromagnetic exchange interactions and spin ground state values  $S = 6^{1/2}$  and  $5^{1/2}$  respectively that are among the largest ones for high nuclearity metal clusters.<sup>[7,22-24,29]</sup> Complex **1** was also found to behave as SMM being the second largest Mn cluster and homometallic SMM reported in the literature.<sup>[1]</sup> It should be pointed out that although compounds containing the  $[Mn^{II}_6Mn^{III}_4(\mu_4-O)_4]^{18+}$  supertetrahedral core are often found to display entirely ferromagnetic exchange interactions and the maximum possible spin ground states,<sup>[19-22,24]</sup> this is not the case for **1** and **2** for which the corresponding maximum values would be, by far, record values of  $S = 209/2$  and  $105/2$ , respectively. Obviously in the case of these two compounds, apart from the exchange interactions within the decametallc supertetrahedral core, which are expected to be ferromagnetic, there are also additional ones between the neighbouring  $M_{10}$  repeating units some of which are antiferromagnetic. For this reason, although dominant ferromagnetic behaviour was realized for both complexes the spin ground states observed are significantly lower than the maximum possible values. However, these magnetic systems have the potential to display larger  $S$  values if some of the antiferromagnetic interactions are switched to ferromagnetic ones by synthesizing analogues of **1** and **2** with slightly different bond lengths and angles, peripheral ligation, etc., as was accomplished in the past for other magnetic systems.<sup>[29]</sup> Thus, **1** and **2** could prove to be stepping-stones towards the construction of new families of materials with abnormally high spin ground states. These compounds are also the first molecular species containing more than two repeating decametallc supertetrahedra and their cores are related to each other and also to that of the  $Mn_{17}$  "dimeric" analogues consisting of two edge-sharing decametallc supertetrahedra. Thus, **1** and **2** can be considered as the "octamer" and "tetramer", respectively, of the well – known decametallc supertetrahedra, and their isolation reveals that other molecular oligomers based on a large number of the same, or other, repeating high nuclearity clusters are possible. Synthetic investigations targeting larger analogues of this series of molecular oligomers such as the dodecamer, the hexadecamer, etc are in progress and the results shall be reported in due course. Indisputably, this study opens up new directions in metal cluster chemistry towards the construction of giant metal clusters with fascinating crystal structures and magnetic properties.

## Experimental Section

Full experimental details for the synthesis and characterization of the reported complexes are provided in the supporting information.

**Keywords:** manganese • cluster compounds • magnetic properties • O ligands • single-molecule magnets

## Acknowledgements

This work was supported by the Cyprus Research Promotion Foundation Grant "ANABAΘMISHTH/ΠAΓIO/0308/12" which is co-funded by the Republic of Cyprus and the European Regional Development Fund, the US National Science Foundation (Grant DMR-1213030 to G.C.) and the Spanish MINECO (Project FEDER-MAT2012-38318-C03-01).

- [1] A. J. Tasiopoulos, A. Vinslava, W. Wernsdorfer, K. A. Abboud, G. Christou, *Angew. Chem. Int. Ed.* **2004**, *43*, 2117-2121.
- [2] E. E. Moushi, C. Lampropoulos, W. Wernsdorfer, V. Nastopoulos, G. Christou, A. J. Tasiopoulos, *J. Am. Chem. Soc.* **2010**, *132*, 16146-16155.
- [3] R. T. W. Scott, S. Parsons, M. Murugesu, W. Wernsdorfer, G. Christou, E. K. Brechin, *Angew. Chem. Int. Ed.* **2005**, *44*, 6540-6543.
- [4] S. K. Langley, R. A. Stott, N. F. Chilton, B. Moubarak, K. S. Murray, *Chem. Commun.* **2011**, *47*, 6281-6283.
- [5] M. Manoli, R. Inglis, M. J. Manos, V. Nastopoulos, W. Wernsdorfer, E. K. Brechin, A. J. Tasiopoulos, *Angew. Chem. Int. Ed.* **2011**, *50*, 4441-4444.
- [6] T. Liu, Y.-J. Zhang, Z.-M. Wang, S. Gao, *J. Am. Chem. Soc.* **2008**, *130*, 10500-10501.
- [7] S. Kang, H. Zheng, T. Liu, K. Hamachi, S. Kanegawa, K. Sugimoto, Y. Shiota, S. Hayami, M. Mito, T. Nakamura, M. Nakano, M. L. Baker, H. Nojiri, K. Yoshizawa, C. Duan, O. Sato, *Nat. Commun.* **2015**, *6*, 5955-5960.
- [8] P. Alborés, E. Rentschler *Angew. Chem. Int. Ed.* **2009**, *48*, 9366-9370.
- [9] M. Murugesu, R. Clérac, C. E. Anson, A. K. Powell, *Inorg. Chem.* **2004**, *43*, 7269-7271.
- [10] F. Xu, H. N. Miras, R. A. Scullion, D.-L. Long, J. Thiel, L. Cronin, *PNAS* **2012**, *109*, 11609-11612.
- [11] J.-B. Peng, X.-J. Kong, Q.-C. Zhang, M. Orendáč, J. Prokleška, Y.-P. Ren, L.-S. Long, Z. Zheng, L.-S. Zheng, *J. Am. Chem. Soc.* **2014**, *136*, 17938-17941.
- [12] M. Charalambous, E. E. Moushi, C. Papatrifiatyllopoulou, W. Wernsdorfer, V. Nastopoulos, G. Christou, A. J. Tasiopoulos, *Chem. Commun.* **2012**, *48*, 5410-5412.
- [13] W.-G. Wang, A.-J. Zhou, W.-X. Zhang, M.-L. Tong, X.-M. Chen, M. Nakano, C. C. Beedle, D. N. Hendrickson, *J. Am. Chem. Soc.* **2007**, *129*, 1014-1015.
- [14] G. F. S. Whitehead, F. Moro, G. A. Timco, W. Wernsdorfer, S. J. Teat, R. E. P. Winpenny, *Angew. Chem. Int. Ed.* **2013**, *52*, 9932-9935.
- [15] X.-J. Kong, L.-S. Long, R.-B. Huang, L.-S. Zheng, T. D. Harris, Z. Zheng, *Chem. Commun.* **2009**, 4354-4356.
- [16] X.-J. Kong, Y.-P. Ren, W.-X. Chen, L.-S. Long, Z. Zheng, R.-B. Huang, L.-S. Zheng, *Angew. Chem. Int. Ed.* **2008**, *47*, 2398-2401.
- [17] J.-D. Leng, J.-L. Liu, M.-L. Tong, *Chem. Commun.* **2012**, *48*, 5286-5288.
- [18] G. F. S. Whitehead, J. Ferrando-Soria, L. G. Christie, N. F. Chilton, G. A. Timco, F. Moro, R. E. P. Winpenny, *Chem. Sci.* **2014**, *5*, 235-239.
- [19] T. C. Stamatatos, K. A. Abboud, W. Wernsdorfer, G. Christou, *Angew. Chem. Int. Ed.* **2006**, *45*, 4134-4137.
- [20] M. Manoli, R. D. L. Johnstone, S. Parsons, M. Murrie, M. Affronte, M. Evangelisti, E. K. Brechin, *Angew. Chem. Int. Ed.* **2007**, *46*, 4456-4460.

- [21] S. Nayak, M. Evangelisti, A. K. Powell and J. Reedijk, *Chem. Eur. J.* **2010**, *16*, 12865-12872.
- [22] E. E. Moushi, T. C. Stamatatos, W. Wernsdorfer, V. Nastopoulos, G. Christou, A. J. Tasiopoulos, *Inorg. Chem.* **2009**, *48*, 5049–5051.
- [23] S. Nayak, L. M. C. Beltran, Y. Lan, R. Clérac, N. G. R. Hearn, W. Wernsdorfer, C. E. Anson, A. K. Powell, *Dalton Trans.*, **2009**, 1901-1903.
- [24] A. M. Ako, I. J. Hewitt, V. Mereacre, R. Clérac, W. Wernsdorfer, C. E. Anson and A. K. Powell, *Angew. Chem., Int. Ed.*, **2006**, *45*, 4926-4929.
- [25] Crystallographic data for 1·10DMF and 2·DMF are provided in the supporting information. CCDC 1422256 and 1422257 contain the supplementary crystallographic data for this paper. These data can be obtained free of charge from The Cambridge Crystallographic Data Center via [www.ccdc.cam.ac.uk/data-request/cif](http://www.ccdc.cam.ac.uk/data-request/cif).
- [26] W. Liu, H. H. Thorp, *Inorg. Chem.* **1993**, *32*, 4102-4105.
- [27] I. D. Brown, D. Altermatt, *Acta Crystallogr. Sect. B* **1985**, *41*, 244-247.
- [28] M. Evangelisti in "Molecule-based magnetic coolers: Measurement, design and application", (Eds.: J. Bartolomé, F. Luis and J. F. Fernández), *Molecular Magnets, NanoScience and Technology*, Springer-Verlag, Berlin, Heidelberg, **2014**, pp. 365-387.
- [29] T. C. Stamatatos, K. A. Abboud, W. Wernsdorfer, G. Christou, *Angew. Chem. Int. Ed.* **2007**, *46*, 884 – 888.
-

